Solar Energy Materials & Solar Cells 117 (2013) 544–548

Contents lists available at ScienceDirect

Solar Energy Materials & Solar Cells

journal homepage: www.elsevier.com/locate/solmat

Versatile electrowetting arrays for smart window applications-from small to large pixels on fixed and flexible substrates

H. You, A.J. Steckl *

Nanoelectronics Laboratory, Department of Electrical Engineering and Computing Systems, University of Cincinnati, Cincinnati, OH 45221-0030, USA

ARTICLE INFO

Article history:
Received 20 April 2013
Received in revised form
20 July 2013
Accepted 22 July 2013

Keywords:
Smart window
Electrowetting
Array
Switching

ABSTRACT

Versatile electrowetting (EW) arrays were fabricated with small to large pixels, on fixed glass and flexible polymer substrates, for smart window applications. EW prototypes on glass substrates were constructed with pixel sizes ranging from 50 μm × 150 μm to 2 mm × 2 mm. The dosing of the array with colored oil was achieved by dip coating the substrate through an oil film suspended on a water bath. The arrays can be driven by either DC or AC voltage. Optical transmission of the prototypes can be modulated from ~5% to > 70% with a relatively low applied voltage of ~15 V. The switching speed of the prototype depends on oil properties and cell size, typically ~10 ms for 300 μm × 900 μm pixel cells. Flexible color EW array prototypes have been fabricated on polymer polyethylene terephthalate (PET) substrates, which can be switched reversibly by applying a relatively low voltage difference between the water and bottom electrode. The EW specifications are maintained even when the prototype is mechanically flexed. These results indicate the promise of EW technology for smart window applications.

1. Introduction

Increases in energy consumption and issues of global warming and environment pollution are increasing the consideration of energy efficiency in industry, transportation, and residential design, among others. The windows of a house, building and automobile represent one of the least energy-efficient components. A new class of windows called “smart windows” or “dynamic tintable windows” has been attracting rapidly increased attention [1–3], owing to their potential to change optical properties, such as the solar factor and the transmission of radiation in the solar spectrum, in response to electric voltage or current or to change by environmental conditions like solar radiation (photochromic) or temperature (thermochromic). The use of smart windows may drastically reduce the energy consumption of buildings by reducing cooling and heating loads and the demand for electrical lighting. Various technologies are used in smart windows, such as chromic materials [4], liquid crystals [5], and electrophoretic or suspended-particle devices [6]. Smart window products based on these technologies are becoming available in the market. One of the shortcomings of current technologies is long switching time for coloration and bleaching [7]. This issue is likely to become even more serious as the size of devices increases to cover larger windows. Another important consideration for future smart windows is the development of ultra-thin and flexible products to be used in curved glass windows. Finally, the durability of smart windows is also crucial.

The electrowetting (EW) effect [8,9] provides an interesting approach for smart windows, through the modification of the wetting properties of a hydrophobic surface with an applied electric field. The EW effect can provide rapid manipulation of two immiscible liquids (one of which is clear and the other containing dye) on a micrometer scale [10]. EW has a number of interesting applications which have recently been developed, such as optical filters, [11] adaptive lens systems, [12] and lab-on-chip [13] in addition to reflective displays [8,14]. Compared with other technologies, the EW technology has several advantages: switching speeds in millisecond range, wide viewing angle and relatively low power consumption [15].

In this work, versatile EW arrays consisting of a range of small (50 μm × 150 μm) to large (2 mm × 2 mm) pixels fabricated on polymer and glass substrates are reported for smart window applications. The optical transmission of the prototypes in the visible range is demonstrated. Flexible EW smart window prototypes are fabricated and the flexible operation is demonstrated at a relatively low voltage.

2. Materials and methods

The single color EW array device structure illustrated in Fig. 1a consists of a dielectric-covered transparent bottom electrode on the glass substrate, a hydrophobic insulator layer (Cytop CTL-809M),

* Corresponding author at: 839 Rhodes Hall, University of Cincinnati, OH 45221, USA. Tel.: +1 513 556 4777; fax: +1 513 556 7326.
E-mail address: a.steckl@uc.edu (A.J. Steckl).

0927-0248/$ - see front matter © 2013 Elsevier B.V. All rights reserved.
http://dx.doi.org/10.1016/j.solmat.2013.07.027

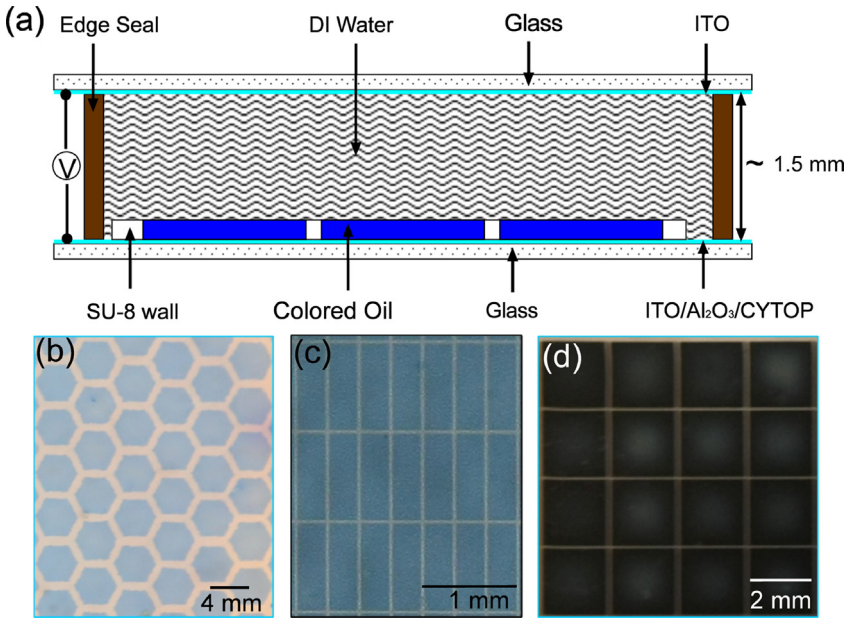

Fig. 1. Single-color EW arrays on glass substrates: (a) schematic diagram of device structure; photographs of several arrays; (b) 2 mm hexagonal (blue) pixel; (c) 300 μm × 900 μm rectangular (blue) pixel; and (d) 2 mm × 2 mm square (black) pixel. (For interpretation of the references to color in this figure legend, the reader is referred to the web version of this article.)

a hydrophilic grid (SU-8 photoresist), the two fluids (water and oil), and the top electrode (ITO/glass). Details of the device fabrication process have been previously described [16,17]. The active device area is defined by the hydrophilic grid, which confines the oil by strongly attracting the water. When a negative bias is applied to the water droplet, the resulting field across the hydrophobic insulator effectively increases its surface energy and reduces its hydrophobicity, attracting the polar water molecules to the insulator surface. With increasing bias, the water increasingly displaces the oil layer to the side of the pixel. Fig. 1b, c and d shows zoom-in photographs of assembled color EW arrays with different pixel sizes and shapes.

For the flexible prototype, the device structure is illustrated in Fig. 2a. A 175 μm thick polyethylene terephthalate (PET) was used as the substrate. The hydrophobic insulator (Cytop) and the underlying insulator layers (Parylene C) are typically 100 nm and 1 μm thick, respectively. A ~8 μm high hydrophilic grid uses epoxy-based negative photoresist (SU-8 2010) to confine the oil film in each pixel. All of the processes on the PET substrate were carried out below 150 °C to prevent degradation of the PET film. Multi-element (~1000–2000) arrays with pixel sizes of 200 μm × 600 μm and 300 μm × 900 μm were fabricated. The width of the hydrophilic grid is 25 μm for both arrays. Fig. 2b shows magnified photographs of each layer of the three color arrays (300 μm × 900 μm pixel size) before final assembly of the overall EW device.

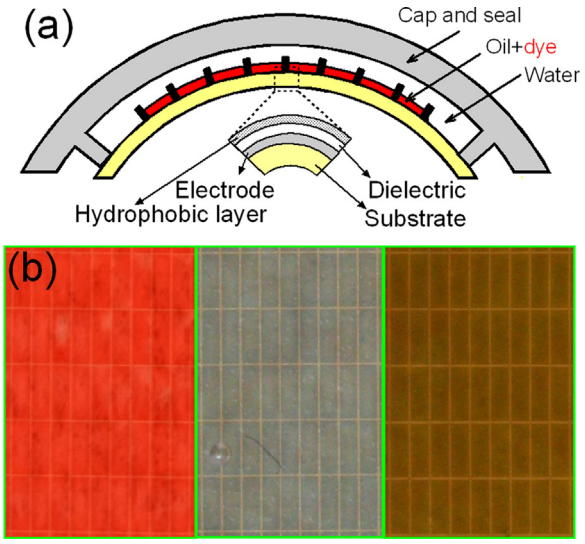

Fig. 2. Color EW array using flexible PET substrate: (a) schematic diagram of device structure and (b) high magnification view of 9 × 5 section of arrays with 300 μm × 900 μm pixels.

3. Results and discussion

3.1. Large pixel array characteristic on fixed glass substrates

The pixel switching process in a typical EW array is illustrated in Fig. 3, which shows a 10 × 10 array with pixel dimensions of 1.5 mm × 1.5 mm from closed to open states under applied AC voltage of 14 V RMS. The process is reversible and can be repeated for many cycles. Moreover, early prototype modules are still fully operable for over 2 years so far. For these square geometry pixels, the black oil is displaced to the four corners of each pixel when the voltage is applied. For rectangular pixels, the oil is displaced to the long sides of the rectangle when voltage is applied.

This control depends on the array configuration and the properties of grid materials used in the array, which control the oil profile in the pixel (concave vs. convex). If the oil is pinned at the edge of the grid with a convex profile, the oil will be displaced to the center of the pixel when voltage is applied [18]. If the oil is pinned to the edge of the grid with a concave profile, the oil will be displaced to the corners of the pixel. The electromechanical force will break the oil first at its thinnest location, namely in the center (corner) of the pixel in the concave (convex) oil profile.

The full spectrum electro-optic characteristics of a fixed array prototype with black oil were obtained by measuring the transmission over the visible range with and without applied voltage. As shown in Fig. 4a, under zero bias the low surface tension black oil preferentially covers the low surface energy hydrophobic

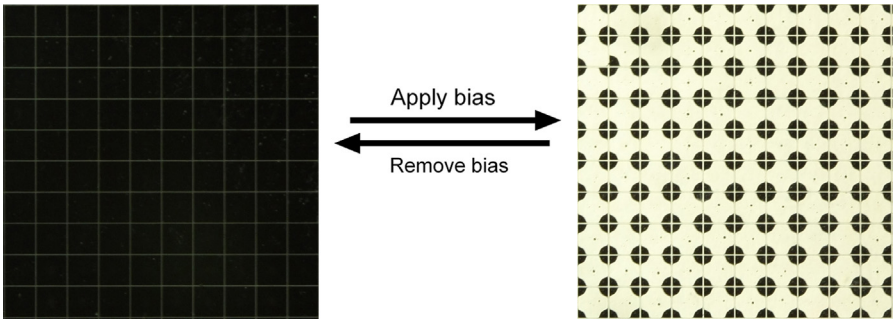

Fig. 3. EW switching of 10 × 10 array with 1.5 mm × 1.5 mm pixels: (left) zero bias and (right) 14 V (RMS), 1 kHz.

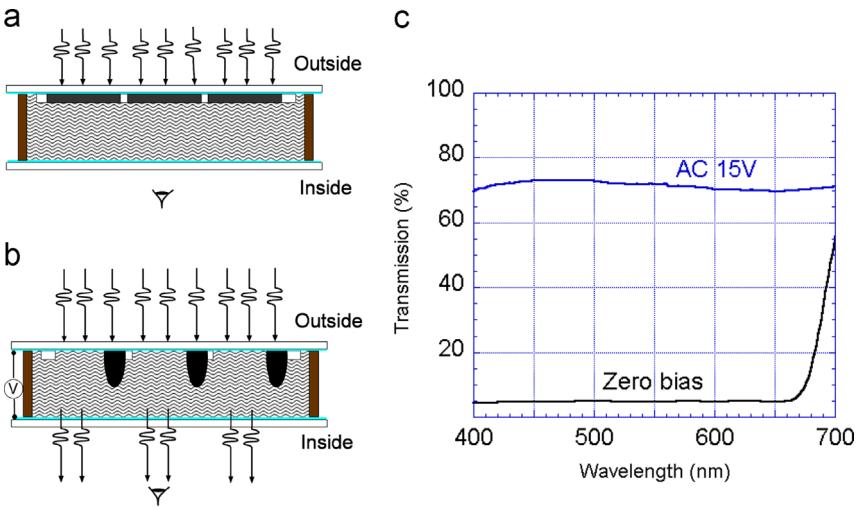

Fig. 4. Optical characteristics of EW arrays (20 × 20 pixels, pixel size: 1.5 mm × 1.5 mm) on glass: (a) schematic at zero bias; (b) schematic with bias; and (c) transmission over the visible range at zero bias and with 15 V RMS 1 kHz bias.

insulator, forming a thin film that excludes the high surface tension water. Consequently, the array shows very low transmission. As bias is applied, the black oil is displaced to the side region of each pixel, hence increasing the clear fraction of each pixel area, thus resulting in higher optical transmission for the array, as shown in Fig. 4b. A representative example of the change in transmission is shown in Fig. 4c. A sample consisting of two glass substrates with a water layer in between was used as a reference. A black EW array (20 × 20 pixels, pixel size: 1.5 mm × 1.5 mm) using 4 wt% black dye in tetradecane oil has a zero bias transmission of ~5%. When a voltage of 15 V RMS (1 kHz) is applied, the transmission increases dramatically to 70%. The transmission in the "off" state can be decreased to nearly 0% by increasing the oil volume dosed in the pixel arrays (by increasing the height of the SU-8 grid) or increasing the dye concentration. The "on" state is realized by applying a voltage through the water medium. The open ("clear") area is controlled by the driving voltage. Therefore, the effect of dye concentration on the transmittance will be minor. At higher voltages, it can be expected that up to 90% of the pixel can be exposed, resulting in very high transmission. In addition to the driving voltage, the dye concentration in oil, the volume of the oil and the pixel geometry can affect the optical transmission.

3.2. *Small pixel array Characteristics on flexible polymer substrate*

Smart window prototypes on flexible PET substrates of EW arrays (45 × 21 pixels, 300 μm × 900 μm pixel area) of different colors are shown in Fig. 5 in both "off" and "on" states. As seen in the photographs, the arrays are being mechanically flexed during operation. The top row of photographs shows the blue, green and red arrays in the "off" state (at zero bias). As the bias voltage (1 kHz AC) is increased beyond a small threshold voltage, the oil in the pixels of each array begins to contract. Beyond threshold, the open (oil-free) area of the cells increases with increasing bias voltage. This indicates that the voltage-controlled transmission modulation can be realized with these prototypes. A driving voltage of 20 V RMS results in ~80% open area for all three prototypes, as shown in Fig. 5b, d, and f. At higher voltages (~30 V), up to 90% open area can be reached.

The spectral electro-optic characteristics of a flexible array prototype with black oil were obtained by measuring the transmission at visible wavelengths (400–700 nm), as shown in Fig. 6. Results obtained with an identical array on a glass substrate are included for comparison. With pixels in the "off" state, the transmission of the PET prototype was ~20 ± 5% higher than that of the glass prototype which was ~12 ± 3%. Increasing the oil volume dosed in the pixel arrays (by increasing the height of the SU-8 grid) can decrease the transmission in the "off" state to nearly 0%. In the "on" state at a voltage of 20 V RMS, the oil film has contracted dramatically and exposing ~80% of the pixel area. This produced an optical transmission ~65 ± 5% for the EW array on PET, which is actually higher than of the glass prototype (~50%). At higher voltages (~40 V), the transmission has reached a value as high as 90%. However, these high voltages negatively affect the operating lifetime of the arrays.

The optically measured transient response of PET and glass EW prototypes with 300 μm × 900 μm pixels and blue oil is shown in Fig. 7 using a step function bias of 20 V RMS at 1 kHz. The transient process was captured by using a high-speed camera (TSHRMS, Fastec Imaging Corp.) at 1000 fps. The open area fraction increases with time and reaches saturation in ~10–15 ms. The switch-on times (0–90% of saturation value) of the PET and glass prototypes

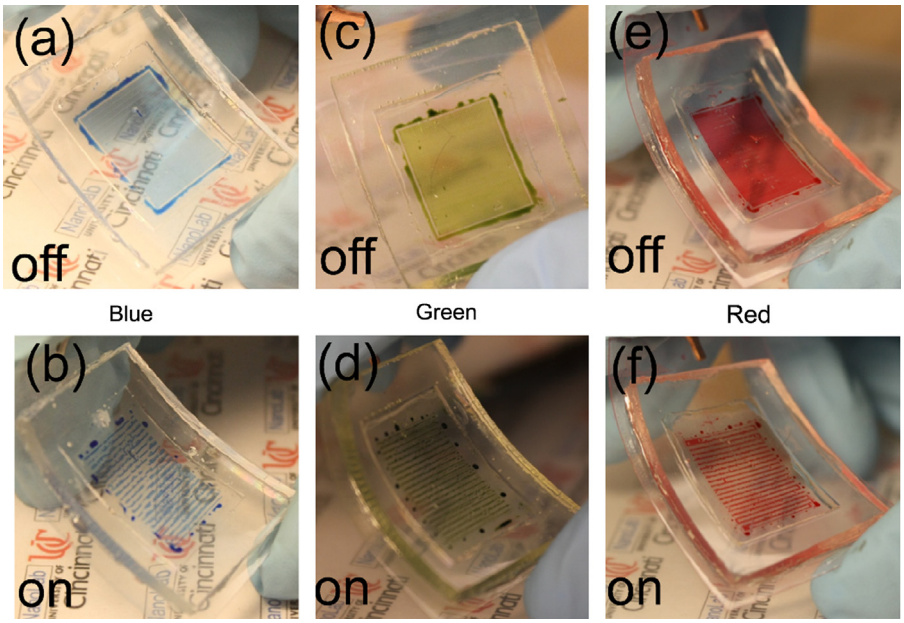

Fig. 5. Photographs of flexible arrays (45 × 21 pixels, pixel size: 300 μm × 900 μm) of three different color devices; top photographs are in the "off" state, bottom photographs are biased into the "on" state with 1 k Hz 20 V RMS driving voltage.

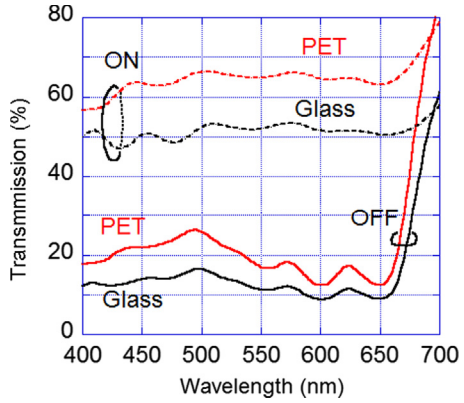

Fig. 6. Transmission spectra of black EW arrays (45 × 21 pixels, pixel size: 300 μm × 900 μm) on PET and glass substrates: off-zero bias and on-20 V RMS 1 kHz.

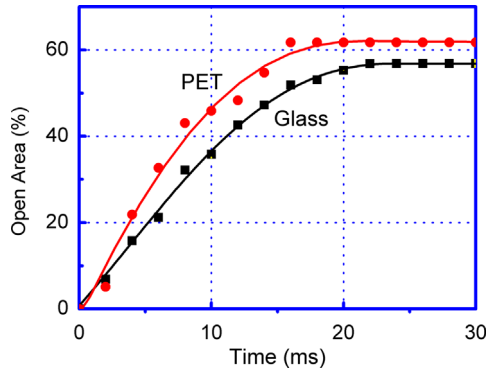

Fig. 7. Switching speed of a single 300 μm × 900 μm pixel on PET and glass substrates, showing the transient response of blue oil open area fraction as a step function bias (20 V RMS, 1 kHz) is applied. The switch-on times (0–90% of saturation value) and standard deviations averaged over 10 separate pixels are 9.6 ± 0.4 ms and 10.6 ± 0.5 ms for PET and glass substrate devices, respectively.

averaged over 10 separate pixels are 9.6 ± 0.4 ms and 10.6 ± 0.5 ms, respectively. This is consistent with other recently reported results [16]. Prototypes with oil of other colors have similar time response characteristics. Since the switch-on process is voltage driven, a faster response can be obtained at higher voltage. This demonstrates that the EW array PET prototypes are suitable for fast switching smart window applications.

3.3. EW array for smart window applications

The smart window applications of the EW prototypes are evaluated through the transmission modulation behavior under various voltages in the range of 0–20 V. It was found that for both stacks, a coloration state (pixel "off" state) was present in the absence of applied voltage, while a bleached state (pixel "on" state) was induced at an applied voltage of 20 V. Fig. 8 shows the switching process for a 3 × 3 cm^2 EW (20 × 20 array with 1.5 mm × 1.5 mm pixels) smart window prototype on glass substrate without and with voltage applied.

It should be pointed out that these EW-based smart windows can operate even in very cold climates. The effect of low temperatures can be mitigated by the addition of salts, ethylene glycol or other additives into the water to prevent freezing.

4. Conclusions

Versatile electrowetting smart window arrays, with small and larger pixels on fixed and flexible substrates, were fabricated and tested. EW array prototypes on fixed glass substrates were constructed with different pixel sizes ranging from 50 μm × 150 μm to 2 mm × 2 mm. The transmission of the prototype can be modulated from ~5% (zero bias) to >70% (~15 V). The device can be driven by either DC or AC voltage. The switching speed depends on the oil properties and cell size, typically ~10 ms for 300 μm × 900 μm pixel cells. Flexible color EW smart window array prototypes have been fabricated on PET substrates with pixel sizes of 300 μm × 900 μm and 200 μm × 600 μm. Flexible EW arrays dosed with oils containing red, green, and blue dyes can be switched reversibly by applying a relatively low voltage difference between the water and bottom electrode. The EW specifications are maintained even when the prototype is mechanically flexed. These results indicate the promise of fixed and flexible EW devices for smart window applications.

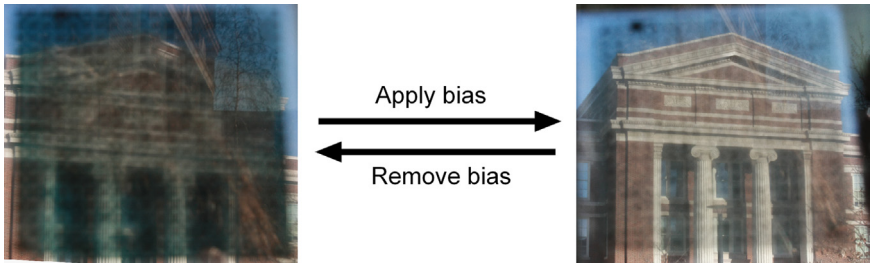

Fig. 8. EW smart window (total size 3 cm × 3 cm; 20 × 20 array with 1.5 mm × 1.5 mm pixel area) in the "off" (zero bias) (left) and "on" conditions (14 V RMS, 1 kHz) (right).

Acknowledgments

Partial support for this project by Raytheon Co., SAPPI Co. and R J Reynolds Co. is gratefully acknowledged. The authors appreciate many useful technical discussions on electrowetting with members of the Nanoelectronics Laboratory and Novel Devices Laboratory at the University of Cincinnati.

References

[1] C.M. Lampert, Smart switchable glazing for solar energy and daylight control, Solar Energy Materials and Solar Cells 52 (1998) 207–221.
[2] C.M. Lampert, Large-area smart glass and integrated photovoltaics, Solar Energy Materials and Solar Cells 76 (2003) 489–499.
[3] R. Baetens, B.P. Jelle, A. Gustavsen, Properties, requirements and possibilities of smart windows for dynamic daylight and solar energy control in buildings: a state-of-the-art review, Solar Energy Materials and Solar Cells 94 (2010) 87–105.
[4] C.G. Granqvist, Electrochromism and Smart Window Design, Solid State Ion 53 (1992) 479–489.
[5] S. Park, J.W. Hong, Polymer dispersed liquid crystal film for variable-transparency glazing, Thin Solid Films 517 (2009) 3183–3186.
[6] R. Vergaz, J.M. Sanchez-Pena, D. Barrios, C. Vazquez, P. Contreras-Lallana, Modelling and electro-optical testing of suspended particle devices, Solar Energy Materials and Solar Cells 92 (2008) 1483–1487.
[7] H. Inaba, M. Iwaku, K. Nakase, H. Yasukawa, I. Seo, N. Oyama, Electrochromic display device of tungsten trioxide and prussian blue films using polymer gel electrolyte of methacrylate, Electrochimica Acta 40 (1995) 227–232.
[8] R.A. Hayes, B.J. Feenstra, Video-speed electronic paper based on electrowetting, Nature 425 (2003) 383–385.
[9] H. You, A.J. Steckl, Lightweight electrowetting display on ultra-thin glass substrate, Journal of the Society for Information Display, http://dx.doi.org/10.1002/jsid.169.
[10] F. Mugele, J.C. Baret, Electrowetting: from basics to applications, Journal of Physics: Condensed Matter 17 (2005) R705–R774.
[11] M.W.J. Prins, W.J.J. Welters, J.W. Weekamp, Fluid control in multichannel structures by electrocapillary pressure, Science 291 (2001) 277–280.
[12] B. Berge, J. Peseux, Variable focal lens controlled by an external voltage: an application of electrowetting, The European Physical Journal E 3 (2000) 159–163.
[13] S.K. Cho, H.J. Moon, C.J. Kim, Creating, transporting, cutting, and merging liquid droplets by electrowetting-based actuation for digital microfluidic circuits, Journal of Microelectromechanical Systems 12 (2003) 70–78.
[14] J. Heikenfeld, K. Zhou, E. Kreit, B. Raj, S. Yang, B. Sun, A. Milarcik, L. Clapp, R. Schwartz, Electrofluidic displays using Young–Laplace transposition of brilliant pigment dispersions, Nature Photonics 3 (2009) 292–296.
[15] R. Shamai, D. Andelman, B. Berge, R. Hayes, Water, electricity, and between: on electrowetting and its applications, Soft Matter 4 (2008) 38–45.
[16] H. You, A.J. Steckl, Three-color electrowetting display device for electronic paper, Applied Physics Letters 97 (2010) 023514.
[17] H. You, A.J. Steckl, Electrowetting on flexible substrates, Journal of Adhesion Science and Technology (2012) 1931–1939.
[18] B. Sun, J. Heikenfeld, Observation and optical implications of oil dewetting patterns in electrowetting displays, Journal of Micromechanics and Microengineering 18 (2008) 025027.